Applied Mechanics and Materials Vol. 82 (2011) pp 100-105
Online available since 2011/Jul/27 at www.scientific.net

doi:10.4028/www.scientific.net/AMM.82.100

Static-Dynamic Properties of Reactive Powder Concrete with Blast Furnace Slag

Huang Hsing Pan[1,a], Jen-Po Peng[1,b],
Yuh-Shiou Tai[2,c] and Chao-Shun Chang[3,d]

[1]Department of Civil Engineering, Kaohsiung University of Applied Sciences, Kaohsiung, Taiwan

[2]Department of Civil Engineering, ROC Military Academy, Kaohsiung, Taiwan

[3]Dept. of Construction Eng., Kaohsiung First University of Sci. & Technology, Kaohsiung, Taiwan

[a]pam@cc.kuas.edu.tw, [b]L656865@hotmail.com, [c]ystai@cc.cma.edu.tw, [d]cschang@nkfust.edu.tw

Keywords: Reactive powder concrete, Slag, Toughness, Seismic resistant property, Strain rate.

Abstract. Reactive powder concrete (RPC) containing blast furnace slag prepared for hydraulic structure with a designed strength of 150 MPa is examined. We first investigate mixture proportions of RPC to fit the strength requirement, and then, concentrate on the material with 50% replacement of silica fume by blast furnace slag to study seismic resistant properties. Results indicate that curing process and steel fiber can enhance the compressive strength, flexural strength, shear strength and fracture toughness. With 210℃ curing, flexural strength of RPC containing 2% steel fibers reaches 91 MPa, almost three times without the fibers. Meanwhile, the shear strength is 47.8 MPa. Dynamic stress-strain curves determined by SHPB test display that the compressive strength of RPC increases with increasing applied strain rate. Applied strain rate dominates the stress-strain behavior and fracture energy of RPC. Toughness index of RPC is improved powerfully by adding a few steel fibers. The fracture toughness of RPC with 50% slag replacement comes to 1.08 MPa·$m^{1/2}$, and reaches 2.67 MPa·$m^{1/2}$ as 2% steel fibers are added.

Introduction

Reactive powder concrete (RPC) compared with normal concrete is considered as an ultra high strength cementitious material with its compressive strength up to 800MPa [1]. Many of RPC's advantages have been reported such as high flexural strength, freeze-thaw resistance, outstanding repair and retrofit potentials, interfacial-toughening effect, low shrinkage and excellent durability [2-6].

Conventional RPC consists of cement, fine aggregate, very fine quartz powders, silica fume and small sized steel fibers [7]. Among those constituents, silica fume is relatively expensive in Taiwan and needs to be imported from others countries. This leads to the undesired high cost in producing RPC. For other countries where silica fume is not economically available, similar problem raised by high cost has limited the practical applications of RPC. Recently, adding fly ash and/or ground granulated blast furnace slag into RPCs as the partial replacement of cement and silica fume has greatly emerged [8-11].

In this study, a specific RPC with blast furnace slag and of a 150 MPa compressive strength is investigated. This target strength is intended for the Taiwan hydraulic structures (embankment, weir and pier) that have experienced tremendous floods during typhoon Morakot in 2009 (2500mm precipitation in two days). Specifically, we utilize blast furnace slag as an alternative silica source for RPC, and explore the static-dynamic properties including stress-strain curves, flexural strength, shear strength, fracture energy, toughness index and fracture toughness. In order to find the fitting mixture ratios, the effects of curing temperature, blast furnace slag and steel fibers are also considered.

Materials

The constituents of RPC are Type II Portland cement (15.8μm), silica fume (SF, with 0.1~0.2μm), slag with Blaine fineness of 6000, quartz powder (5~20μm), quartz sand (200~600μm), and ASTM Type-G superplasticizer (SP). The length and the diameter of steel fiber are 12mm and 0.18mm respectively.

Mixture proportions of RPC are shown in Table 1, where the parentheses in A(0%), B(30%), C(50%), D(70%) and E(100%) materials are referred to slag replacement to silica fume in weight. The Arabic numerals of each material represents volume fraction of steel fibers. For example, C1 means a RPC with 50% of silica fume replaced by slag and 1% steel fibers. According to ASTM C230M-03 for the workability with water-to-binder ratio (w/b) of 0.23~0.28, the flow values of all RPC mixtures were well controlled in between 200mm and 250mm, as depicted in Fig.1.

Table 1. Mixture proportions of RPC [kg/m^3]

material	steel fiber	w/b	water	cement	SF	slag	quartz powder	quartz sand	SP
A0	0%	0.23	180	714	216	0	252	944	36
A1	1%	0.23	180	714	216	0	252	918	36
A2	2%	0.23	180	714	216	0	252	891	36
B0	0%	0.23	180	714	151	65	252	962	36
B1	1%	0.23	180	714	151	65	252	936	36
B2	2%	0.23	180	714	151	65	252	910	36
C0	0%	0.23	180	714	108	108	252	973	36
C1	1%	0.23	180	714	108	108	252	947	36
C2	2%	0.23	180	714	108	108	252	921	36
D0	0%	0.25	186	714	65	151	252	940	48
D1	1%	0.25	186	714	65	151	252	914	48
D2	2%	0.25	186	714	65	151	252	888	48
E0	0%	0.28	214	714	0	216	252	892	50
E1	1%	0.28	214	714	0	216	252	866	50
E2	2%	0.28	214	714	0	216	252	840	50

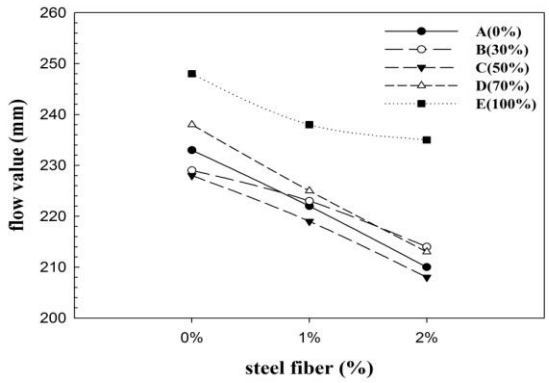

Fig.1 Flow value of RPC

The RPC mixtures were cast into steel moulds and compacted by an iron surcharge. Specimens were stored in room temperature for 2days, removed from the moulds, and then cured in 90℃ water for 7 days (curing 1). In order to consider the curing effect, we also cured RPC specimens in 90℃ water for 5 days, and then, in 210℃ water for 2 days (curing 2) with an additional mark "H" to distinguish RPC from curing 1. For example, the HC1 RPC has the same mixture proportion as C1, but with different curing conditions. After curing, the RPC specimens were placed in the air to dry off for 24 hours before the tests. Specifically, five specimens of each RPC material are prepared for test.

Testing Methods

Specimens with φ50×100 mm were tested for static stress-strain curves with the loading rate of 0.03mm/min (5×10^{-6}/sec) provided by material testing machine MTS 810. The longitudinal and lateral strains were measured by the extensometer. On the other hand, dynamic strain rate tests were performed by using split-Hopkinson pressure bar (SHPB) setting up on the RPC cylinders (φ50×25 mm). The projectile impacts on the Hopkinson bar would develop a compressive longitudinal incident wave. The wave then transmitted into the RPC specimen, and a small part reflected back to the Hopkinson bar due to the difference of impedance. The whole process of wave propagation was recorded via strain gauges and data analyzing apparatus to obtain the dynamic stress-strain curves.

Three-point bending tests were also performed to obtain the flexural strength. It should be mentioned that in this study, toughness index was regarded as the area under the load-deflection curve up to 2mm mid-span deflection according to ASTM C1609. The flexural specimen used in this part was 40×40×160mm, which is smaller than the standard one. The RPC specimens were loaded with the loading rate of 0.06mm/min controlled by MTS 810. The maximum mid-span deflection was set to be 8mm and was recorded by LVDT. The toughness indices T_2, T_4, T_6, and T_8 of RPC specimens were calculated at the deflection level of 2mm, 4mm, 6 mm and 8 mm, respectively.

As for the shear strength of RPC, shear testing was carried out using small push-off specimens with a shear area of 50mm×30mm [12]. Shear specimens were also tested by MTS with a rate of 1 mm/min till the specimen failed. Failure load divided by shear area would then give the shear strength.

The fracture toughness, expressed by the critical stress intensity factor (K_{IC}), was evaluated through three-point bending test with a notch of 4mm in the middle span of specimen in conformity with ASTM E 399. Flexural specimens were tested under the loading rate of 0.02mm/min. From the bending load and the size of the specimen, we can then calculate the critical stress intensity factor.

Results and Discussion

Compressive Strength. The effect of slag replacement and steel fiber to compressive strength at the age of 10 days under curing condition 1 is shown in Fig. 2 (The counterpart RPC, A0, without slag and steel fibers addition has a compressive strength of 150MPa.). Compressive strength goes down with the increasing slag amount in RPC, and up with steel fibers. The compressive strength of E0 material (without silica fume but slag) is 31.28% lower than A0 material. Similarly, E group materials containing 1% and 2% steel fibers marked as E1 and E2 are 33.43% and 30.93% lower than A1 and A2, respectively. Approximately, the compressive strength in group E (0% silica fume and 100% slag) drops one-third as compared with group A (100% silica fume and 0% slag).

Comparisons of the compressive strength at the age of 10 days and 28 days are shown in Figs. 3-5. As shown, the compressive strength for all RPCs increases with the ages except for A1 in Fig.4, whereas the enhancement is not apparent. Both C2 materials (50% silica fume and 50% slag with 2% steel fibers) in Fig. 5 reach the aim of 150 MPa for hydraulic structure. The compressive strength of C mixture proportions under curing condition 1 (90℃ for 7 days) and 2 (90℃ for 5 days and 210℃ for 2 days) is listed in Table 2. The compressive strength at curing 2 (HC group) has a 13~18% increasing as comparing to curing 1 (C group), which almost goes beyond 150MPa. Based on this finding, we then choose C mixture proportions as the required material suitable for hydraulic structures, and continue to explore the material properties.

Table 2. Compressive strength of C mixture proportions [MPa]

curing condition	curing 1			curing 2		
material	C0	C1	C2	HC0	HC1	HC2
compressive strehgth	130	139	156	148	164	184

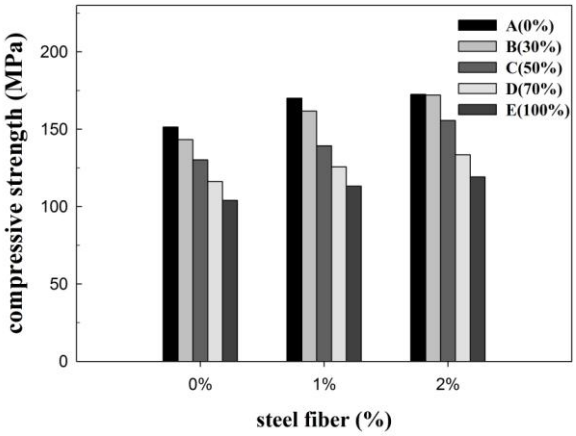

Fig. 2 Effect of slag replacement and steel fibers

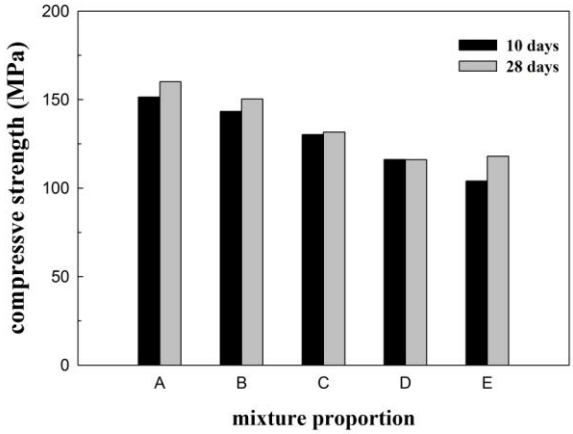

Fig.3 Age effect without steel fibers

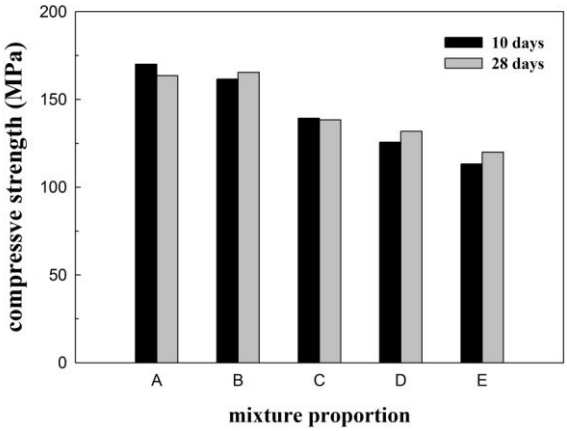

Fig.4 Age effect with 1% steel fibers

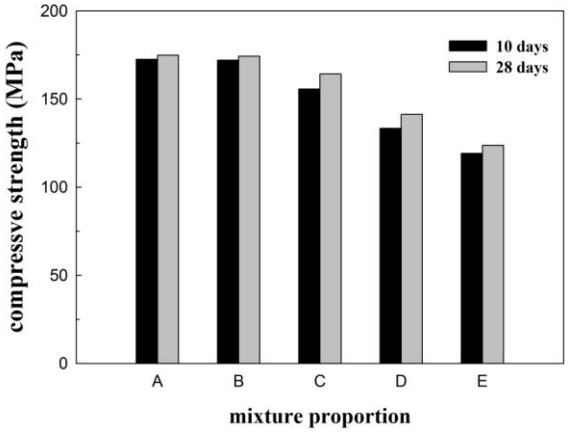

Fig.5 Age effect with 2% steel fibers

Stress-Strain Curves and Fracture Energy. For C mixture proportions, static stress-strain curves of C and HC materials are shown in Figs. 6-7. As seen, HC materials are generally of a more brittle behavior than C materials (such as HC1 in Fig.7 vs. C1 in Fig. 6) while the compressive strength of HC materials is higher.

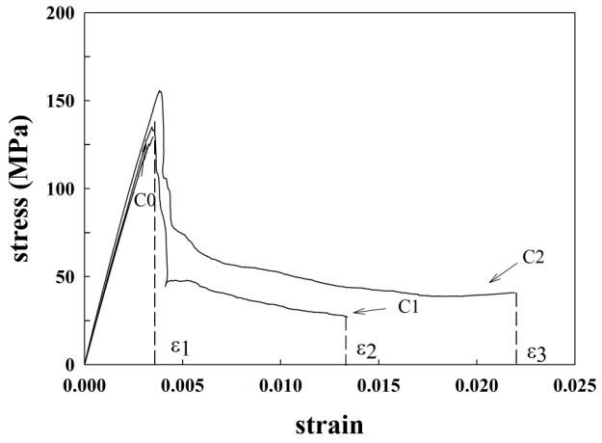

Fig.6 Static stress-strain curve of C materials

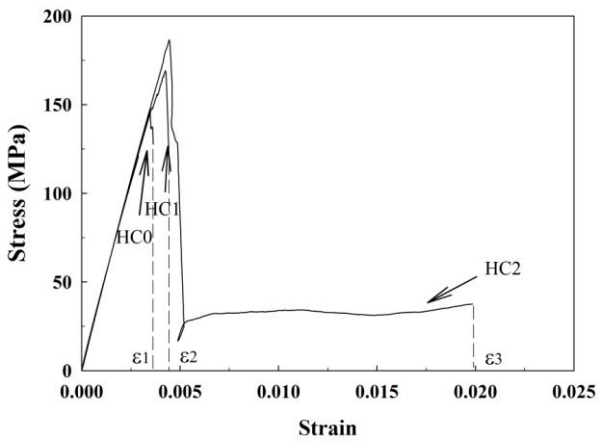

Fig.7 Static stress-strain curve of HC materials

Dynamic stress-strain curves of HC materials determined by SHPB test with three strain rates are shown in Figs. 8-10. It should be noted that the materials subjected to the strain rate below 200/sec did not fail in SHPB test. In Figs. 8-10, the compressive strength increases with the strain rate, and RPC

subjected to the moderate strain rate (476/sec in HC0 and 326/sec in HC1) exhibits the maximum peak strain.

The fracture energy of C and HC materials is shown in Table 3, where ε_1, ε_2 and ε_3 shown in Figs. 6-7 are the maximum strain corresponding to the material with 0%, 1% and 2% steel fibers addition, respectively. In Table 3, the fracture energy for HC0 is somewhat greater than C0, but this will reverse as after steel fibers were added.

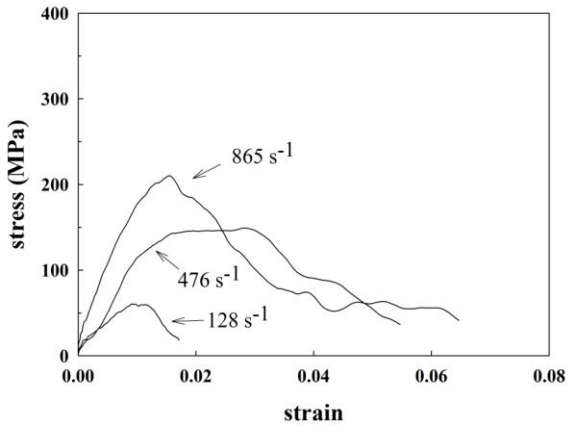

Fig.8 Dynamic stress-strain curve of HC0

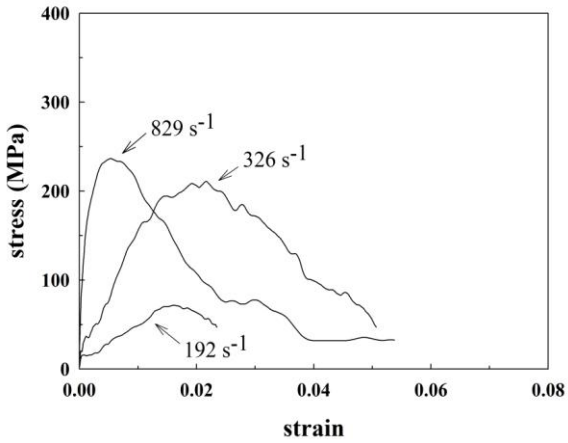

Fig.9 Dynamic stress-strain curve of HC1

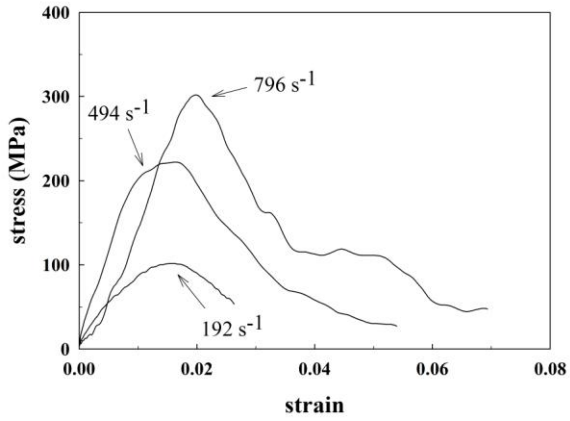

Fig.10 Dynamic stress-strain curve of HC2

Table 3. Fracture energy [MJ/m^3]

material	C0	C1	C2	HC0	HC1	HC2
ε_1	13.6	15.2	17.1	14.1	15.4	15.6
ε_2	–	32.8	44.2	–	20.4	21.1
ε_3	–	–	61.5	–	–	49.7

Flexural Strength and Toughness Index. The flexural strength for C mixture proportions at different curing conditions is displayed in Table 4. As shown, all the flexural strength are developed with increasing the steel fibers contents. The flexural strength of C0 and C1 is greater than that of HC0 and HC1 except for C2 material. Nevertheless, toughness index calculated from the area of load-deflection curve in three-point bending test still shows the same results as the fracture energy presented in Table 3. In other words, the toughness index of C materials with steel fibers (C1 and C2) is higher as comparing to HC materials (HC1 and HC2), as shown in Table 4. For material without steel fibers, this tendency is reversed. For the shear strength, HC material without fibers (HC0) is of 21.73 MPa while HC1 (1% steel fibers) dramatically increases to 44.52 MPa.

Fracture Toughness and Energy Absorption. In Table 4, the critical stress intensity factor (K_{IC}) of C0 and HC0 is 1.08 and 0.611 MPa·m$^{1/2}$ respectively, which is almost three times than that of normal concrete. Fracture toughness grows fast if steel fibers are added into RPC, especially for HC materials. Energy absorption calculated from the area of load-crack opening displacement (P-CMOD) curve is shown in Table 4. For the material containing 2% steel fibers, energy absorption for C2 and HC2 is 2.11 and 5.0 kN-mm respectively, showing a better toughness effect in C mixture proportion.

Table 4. Strength and toughness

material	C0	C1	C2	HC0	HC1	HC2
flexural strength (MPa)	30.57	82.13	88.44	26.20	53.30	91.33
shear strength (MPa)	–	–	–	21.73	44.52	47.80
T_2 (kN-mm)	0.18	20.97	21.57	0.38	10.79	17.42
T_4 (kN-mm)	0.18	30.17	30.59	0.38	16.48	25.64
T_6 (kN-mm)	0.18	33.53	34.20	0.38	19.25	29.39
T_8 (kN-mm)	0.18	35.18	36.03	0.38	20.84	31.43
K_{IC} (MPa·m$^{1/2}$)	1.08	1.86	2.67	0.61	2.37	3.81
energy absorption (kN-mm)	0.17	1.66	2.11	0.55	1.98	5.00

Conclusions

RPC with blast furnace slag as the partial replacement of silica fume is developed to fit the requirement of 150 MPa for hydraulic structures. We conclude the results as follows.

1. The fracture toughness of RPC with 50% slag replacement cured in 90℃ water for 7days comes to 1.08 MPa·m$^{1/2}$, and reaches 2.67 MPa·m$^{1/2}$ as 2% steel fibers are added.
2. With 210℃ curing, flexural strength of RPC containing 2% steel fibers reaches 91 MPa, almost three times without the fibers. Meanwhile, the shear strength is 47.8 MPa.
3. Applied strain rate effectively affects RPC's dynamic stress-strain curve and fracture energy.
4. Steel fiber is more efficient than curing effect in improving RPC's seismic properties and toughness.

Acknowledgments

This study was financially supported by the Taiwan National Science Council under Grant NSC 99-2625-M-151-001. We also thank Mr. Li-Ming Shiau for manufacturing the specimens.

References

[1] P. Richard and M. Cheyrezy: ACI SP144 (1994), p. 507

[2] L. Massidda, U. Sanna, E. Cocco and P. Meloni: ACI SP200 (2001), p. 447

[3] E. Shaheen and N. Shrive: ACI Mater. J. Vol. 103 (2006), p. 444

[4] M.G. Lee, Y.C. Wang and C.T. Chiu: Construct. Build. Mater. Vol. 21 (2007), p. 182

[5] Y.W. Chan and S.H. Chu: Cement Concrete Res. Vol. 34 (2004), p. 1167

[6] C.L.W. Allan, A.C. Paul and B. Richard: Cement Concrete Comp. Vol. 29 (2007), p. 490

[7] P. Richard and M. Cheyrezy: Cement Concrete Res. Vol. 25 (1995), p. 1501

[8] Y. Zhang, W. Sun, S. Liu, C. Jiao and J. Lai: Cement Concrete Comp. Vol. 30 (2008), p. 831

[9] H. Yazici, H. Yigiter, A.S. Karabulut and B. Baradan: Fuel Vol. 87 (2008), p. 2401

[10] H. Yazici, M.Y. Yardimci, S. Aydin and A.S. Karabulut: Construct. Build. Mater. Vol. 23 (2009), p. 1223

[11] H. Yazici, M.Y. Yardima, H. Yigiter, S. Aydin and S. Turkel: Cement Concrete Comp. Vol.32 (2010), p.639

[12] S.G. Millard, T.C.K. Molyneaux, S.J. Barnett and X. Gao: Inter. J. Impact Eng. Vol.37 (2010), p.405.

Performance, Protection and Strengthening of Structures under Extreme Loading
doi:10.4028/www.scientific.net/AMM.82

Static-Dynamic Properties of Reactive Powder Concrete with Blast Furnace Slag
doi:10.4028/www.scientific.net/AMM.82.100